ORIGINAL PAPER

Eventual analysis of global cerebral ischemia-reperfusion injury in rat brain: a paradigm of a shift in stress and its influence on cognitive functions

Sriram Ravindran[1] · Gino A. Kurian[1] ·

Abstract
Cognitive issues in stroke arise as a result of reperfusion of a clogged artery, which is reported to exacerbate the injury in the brain leading to oxidative stress. Through the present work, we try to understand the regional variations across brain regions mainly cortex and striatum associated with the progression of ischemia-reperfusion injury (IRI). In a rat model of IRI, the influence of varying ischemia and reperfusion times on the biochemical phases across the brain regions were monitored. IRI resulted in the blood-brain barrier disruption and developed mild areas of risk. The brain's tolerance towards IRI indicated a progressive trend in the injury and apoptosis from ischemia to reperfusion that was supported by the activities of plasma lactate dehydrogenase and tissue caspase-3. Cognitive impairment in these rats was an implication of cellular oxidative stress (higher lipid peroxidation and lower antioxidant enzyme activity) that persisted by 24-h reperfusion. The oxidative stress was prominent in the cortex than the striatum and was supported by the lower ATP level. Upregulated Mn-SOD expression leading to a preserved mitochondria in the striatum could be attributed to the regional protection. Overall, a progression of IRI was observed from striatum to cortex leading to 5-day cognitive decline.

Introduction

Cerebral ischemia-reperfusion injury (IRI) is a complex and heterogeneous disorder due to factors that dictate the injury such as duration of ischemia, collateral circulations, distal micro-thrombosis, systemic blood pressure changes, age, gender, comorbidities, and finally, genetic predisposition (Bai and Lyden 2015; Kalogeris et al. 2012). The pathophysiology of

✉ Gino A. Kurian
kurian@scbt.sastra.edu

Sriram Ravindran
sriramr@sastra.ac.in

[1] Vascular Biology Laboratory, SASTRA Deemed University, Thanjavur, Tamil Nadu 613401, India

IRI can be divided into the ischemic phase wherein there exists an imbalance between metabolic demand and supply within the ischemic region and the reperfusion phase where there is an activation of inflammatory responses, leading to neurotransmitter firing, endothelial dysfunction causing alterations in the permeability of blood-brain barrier, which is enhanced by ROS production leading to activation of cell death programs (Kalogeris et al. 2012).

Global ischemia of short durations (5 min) to the brain can trigger neuronal death processes in the CA1 region of the hippocampus, which becomes irreversible if extended to 20 min, followed by reperfusion (Baron et al. 2013; Lee et al. 2000). Contrarily, a recent study reported functional restoration even if reperfusion is done after 45 min of ischemia, ascribing to the varying susceptibility of cell types to ischemia, that lead to the recovery within the ischemic area (Tachibana et al. 2017). Hence, oxidative stress experienced in various brain regions is a detrimental factor to assess the damage caused by reperfusion injury, of which hippocampus seemed to be least protected due to reported low levels of

HSP70, antioxidant capacity, and proteasome activity (Garbarino et al. 2015). The observed cell type differences are due to varying degree of redox status within the cells, i.e., their ability to transport reducing equivalents, thiols, nitric oxide, and ascorbates (Bačić et al. 2016) and may be linked to physiologically varying oxygen tensions in mammalian brain (21%, 156 mmHg) regions, with the highest being pia matter (8%, 60 mmHg) and lowest being midbrain (0.55%, 4.1 mmHg) (Erecińska and Silver 2001).

The histological changes post IRI in rat model observed a loss of CA1 neurons from 15 min to 30 min of ischemia (Ordy et al. 1993). Considering that the widely studied model for IRI is rat, there is a limited number of reports encompassing changes related to the injury, inflammation, apoptosis, and oxidative changes over varying time points in the brain, its regions and cell types, specifically in the rat as a model. Although reports on gerbil models are available, their cerebral vascular anatomy is different from rat (Candelario-Jalil et al. 2001; Selakovic et al. 2011). In addition, reperfusion promotes overproduction of reactive oxygen species (ROS) and reactive nitrogen species (RNS), for which the brain is highly sensitive as it causes oxidative stress resulting in memory deficits that occur following stroke (Schimidt et al. 2014). Therefore, in our present investigation, we evaluated the association of injury, oxidative stress, and apoptosis due to IRI with cognitive decline following global cerebral ischemia.

Materials and methods

Experimental animals

All the animal studies were conducted as per the guidelines of the CPCSEA, Government of India, and with the prior approval from the Institutional animal ethical committee (Approval No. IAEC/RPP/298). Male Wistar rats of 230–280 g were used in the study and maintained in individual polycarbonate cages. Feed and water were provided ad libitum and the cages were maintained at 25 ± 2 °C with a relative humidity of ~70%. A 12-h dark/light cycle was followed in the housing. All rats were grouped and acclimatized a week before the start of experimentation.

Induction of cerebral ischemia-reperfusion

The two vessel occlusion model of cerebral ischemia was carried out in the rat as per previously established protocol with slight modifications (Raval et al. 2009). In brief, the rats fasted the night before surgery with free access to drinking water. Anesthesia was induced by inhalation of a mixture of 3.5% halothane in oxygen and maintained at 1.5% during the surgery. A middle incision of the neck was performed. The bilateral common carotid arteries were isolated and loose

threads were placed for subsequent occlusion. A rectal thermometer was inserted through the anus, to monitor the body temperature, which was maintained close to 37 °C by placing the animal on a thermally regulated surgery pad. A pair of needles were inserted into the temporal muscles on the skull to monitor the EEG. Tail arterial blood pressure was monitored using pressure transducer–cannula assembly during surgery as carotid arteries were clamped.

The induction of ischemia was achieved by occluding the bilateral common carotid arteries and the EEG was monitored to confirm occlusion. Isoelectricity of the electroencephalogram was considered as an indication of the onset of ischemia (Li et al. 1999). Additionally, real-time flow was monitored in the vessel using Transonic Nanoprobe (T420) over the vessel until the flow reached 0 mL/min. Ischemia was terminated and reperfusion was ensured by the removal of the carotid clamps.

Reperfusion was maintained till intermediated time points and assigned to ischemic groups of 15 min (I_15) and 30 min (I_30) and reperfusion groups of 15 min (I_30/R_15), 30 min (I_30/R_30), 4 h (I_30/R_4), and 24 h (I_30/R_24) reperfusion following 30 min of ischemia. Rats belonging to groups beyond 30 min of reperfusion were sutured and recovered for spontaneous breathing and maintained in individual cages. A sham group was kept as control which underwent a procedure similar to test groups except that the carotid arteries were not occluded.

Assessment of brain injury

After the assigned duration of ischemia and reperfusion, rats were euthanized by an excess of halothane. The blood and brain were collected to assess the injury. Blood plasma and brain tissue were analyzed for injury markers: lactate dehydrogenase (LDH) and creatine kinase-BB (CK-BB). LDH estimation was based on the lactate conversion to pyruvate and estimated from the formation of NADH measured at 340 nm. CK-BB was estimated by immune-inhibition method as per the kit instructions from Agappe diagnostics, Switzerland (#11405007).

Evaluation of blood-brain barrier (BBB) dysfunction

The integrity of BBB was assessed using two inert tracers: Evans blue and sodium fluorescein according to the established protocol (Yen et al. 2013). Both the dyes were prepared as a 2% solution in 0.9% saline and infused through the tail vein, 30 min prior to the excision of the brain. Rats were anesthetized with halothane as mentioned in the "Induction of cerebral ischemia-reperfusion" section and perfused with saline (200 mL) through the abdominal aorta to wash off excess dye along with the blood and the brain was collected. The extravasated dye was extracted from the homogenized brain using 1:3 volume of 50% TCA, and the

supernatants were diluted with 1:3 volume of 95% ethanol prior to measuring fluorescence at 620 nm/680 nm for Evans blue and 440 nm/525 nm for sodium fluorescein.

Estimation of ATP level by luminescence assay

The brain tissue was frozen in liquid nitrogen immediately after collection and homogenized in mitochondria isolation buffer (250 mM sucrose, 1 mM EGTA, 10 mM HEPES, 0.5% BSA at pH 7.4) under ice-cold conditions in crushed ice. The homogenate was centrifuged at 2000g for 10 min at 4 °C followed by a collection of the supernatant. The supernatant (cytosolic fraction) was used for ATP estimation after pelleting down the mitochondria at 10000g for 10 min at 4 °C (Lai et al. 1977). The level of ATP from the brain regions was estimated using the ATPlite kit from PerkinElmer (USA). Briefly, 50 μL of the cytosolic fraction was added to the lysis buffer and shaken for 10 min followed by addition of substrate buffer and incubated for 10 min. The luminescence signal was recorded at the end of 1-h incubation using Synergy H1 Multimode reader (BioTek, USA).

mRNA expression analysis

The total RNA extraction from brain tissue was carried out separately for cortex and striatum using Trizol reagent (Thermo-Scientific, USA). The reverse transcription was carried out using Verso cDNA synthesis kit (Thermo-Scientific, USA). The expression of mRNA was checked in real time for CuZn-SOD (F-CGGATGAAGAGAGGCATGTT, R-CAATCACACCACAAGCCAAG) and Mn-SOD (F-CCAAGCTAGGCTCCTGACTG, R-TGTTGGACACCGCACTGTAT) using qPCR from Applied Biosystems (ABI-7500). All the expression data was generated in triplicates for each sample and fold expression was calculated by $\Delta\Delta$ Ct method using beta-actin (F-TGACGATATCGCTGCGCTC, R-CAGTTGGTGACAATGCCGTG) as house-keeping gene.

Behavioral study

Radial arm maze

The eight-arm radial maze was used for behavioral testing. The maze was made of wood and kept at an 80-cm elevation from the ground with visual clues available at the end of the arm. In brief, the maze study was performed on rats that were fasted overnight and fed on normal diet mixed with chocolate grain flakes (chocos) after study. The rats were trained for 4 days prior to induction of ischemia-reperfusion injury. Out of eight arms, four arms were baited with chocos and the rest remained unbaited. The rats were allowed to explore and reach the bait within a 10-min window. Three trials were conducted for each rat in a day. Each trial started by placing the rat onto the central region of the maze and assessing the arm entries. The session lasted 10 min to monitor the correct entries and the Working Memory Index (WMI) was calculated by dividing the number of first entries into the baited arms by total entries into the arms with bait. The study consisted of three groups (6 rats/group); sham, ischemia 15 min, and ischemia 30 min followed by reperfusion and behavior assessment for 5 days. The movement of a rat in the maze was recorded using a video camera and used for analysis.

Morris water maze

Spatial learning and memory were performed in the Morris water maze adopting standard procedures with slight modification (Gehring et al. 2015). The water maze consisted of a fiberglass pool of 2 m diameter with a platform of 15 cm diameter submerged just 1 cm below the water surface. The water in the tank was made opaque with milk so as to hide the platform. The pool was surrounded by distal visual cues and kept in a uniformly illuminated room. A digital video recorder suspended above the center of the pool was used to record the swim paths of the animals and video output was digitized for analysis by using SMART 3.0 video tracking software from Panlab (USA). Before the induction of ischemia, rats were trained for 4 consecutive days with 3 trials per day. The main test was conducted after 24 h of reperfusion for 5 days. During each trial, rats were allowed to swim until they found the hidden platform. Rats that failed to find the hidden platform in 90 s were guided to the platform. The parameters computed for analysis among the groups included the average latency time and swimming speed.

Apoptosis detection in the brain regions

The two brain regions comprising of the striatum and cortex were separated by adopting standard procedure (Chinopoulos et al. 2011). After excision, the tissues were used for detection of apoptosis by estimating the caspase-3 activity based on the fluorogenic substrate as per the previous protocol (Gilbert et al. 2016). Briefly, the tissue homogenate was added to the buffer containing HEPES 100 mM, EDTA 0.5 mM, DTT 5 mM, glycerol 20%, CHAPS 0.1%, and substrate 25 μM and the fluorescence (365/465 nm) was monitored for 1 h at 37 °C.

Measurement of inflammatory activity in the brain

The myeloperoxidase (MPO) enzyme activity which is a prominent pro-inflammatory mediator implicated in IRI was determined as described previously (Pulli et al. 2013). Briefly, 10 μl homogenate was added to 80 μl 0.75 mM H_2O_2 and

110 μl tetramethylbenzidine (TMB) solution (2.9 mM TMB in 15% DMSO and 100 mM sodium phosphate buffer maintained at pH 5.4) and incubated at 37 °C for 5 min. The reaction was stopped by adding 50 μl 2 M H_2SO_4, and its absorption was measured at 450 nm to estimate MPO activity.

Assessment of lipid peroxidation and oxidative stress

The brain cytosolic fraction and mitochondria isolated as per the method in the "Estimation of ATP level by luminescence assay" section were used for the estimation of oxidative stress based on lipid peroxidation by quantification of thiobarbituric acid reactive species (TBARS) assay (Ohkawa et al. 1979), reduced glutathione (GSH) (Shaik and Mehvar 2006), and cytosolic enzyme activities such as superoxide dismutase (SOD) (Nandi and Chatterjee 1988), catalase (Li and Schellhorn 2007), glutathione peroxidase (GPx), and glutathione reductase (GR) (Sedlak and Lindsay 1968) were assessed as per standard procedures.

Statistical analysis

The data were analyzed based on the assumption of the normal Gaussian distribution. A one-way analysis of variance (ANOVA) was used for between-group comparison and Dunnet's test was done for multiple comparisons. For behavioral analysis, a two-way ANOVA was used for comparison across the time points between the groups and Tukey test was done for multiple comparisons. The data were presented as mean ± SEM. Values of $P < 0.05$ were considered for statistical significance. The data were analyzed using Graph Pad Prism 7.0.

Results

Induction and progression of injury and apoptosis in cerebral ischemia-reperfusion

The induction of ischemia by occlusion of bilateral carotid arteries was confirmed by isoelectric EEG as shown in Fig. 1a and no real-time blood flow was measured by flow probe in Fig. 1b.

Figure 2 shows injury as assessed in plasma from the activities of LDH and CK-BB and in brain tissue from LDH in the regions of cortex and striatum. Compared to sham, all the groups had elevated levels of these markers in plasma which remained significant ($P < 0.05$) at 24 h of reperfusion compared to sham. The highest ($P < 0.05$) plasma LDH activity was observed at 4 h and 24 h of reperfusion compared to sham (Fig. 2a), the possible source of which is from brain regions that had lower activity at the specific time points (Fig. 2c, d). Significant ($P < 0.05$) area at risk was quantified by TTC

staining and observed to be maximum at 30 min reperfusion followed by 30 min ischemia compared to sham (Online resource 1).

In the present model of IRI, striatum along with the hippocampus remains the most vulnerable region to be affected by ischemia. The apoptotic activity in these brain regions was evaluated from the active caspase-3 measurement (Fig. 3). The cortex showed significantly ($P < 0.05$) higher caspase-3 activity at 4 h and 24 h of reperfusion compared to sham. In case of the striatum, a time point dependent significant ($P < 0.05$) rise in caspase-3 activity was noted from 15 min reperfusion which peaked at 4 h and by 24 h the activity remained just the same as that of 30 min of reperfusion (Fig. 3b).

Impact of ischemia-reperfusion on disruption of blood-brain barrier and progression of inflammation

Ischemia is well known to cause BBB disruption with increasing duration of ischemia. The entry of low molecular weight substances was measured by sodium fluorescein tracer concentrations in the ischemic brain tissue, while the high molecular weight ones were evaluated from the entry of Evans blue. By 15 min of ischemia, significant ($P < 0.05$) amount of low molecular weight protein could be detected and persisted until 24-h reperfusion (Fig. 4a). On the other hand, high molecular weight proteins were significantly ($P < 0.05$) detected only at 15 min of reperfusion and persisted until 24-h reperfusion compared to sham (Fig. 4b).

The myeloperoxidase activity revealed the pro-inflammatory environment in the brain regions (neutrophil infiltration), which seemed elevated significantly ($P < 0.05$) from 15 min ischemia in striatum (Fig. 4d) and only at reperfusion (30 min) in cortex (Fig. 4c) and seemed to subside by the end of 24 h compared to sham.

Oxidative stress changes in brain regions across the tissue and its mitochondria

Lipid peroxidation, imbalances in glutathione cycle, and declined activities of antioxidant enzymes are some of the devastating features of ischemia-reperfusion injury. Collectively termed as oxidative stress, these features are not only confined to cytosol but also are spread across the organelle mainly mitochondria. Table 1 presents the lipid peroxidation levels and GSH content in the cytosol and mitochondria from the cortex and striatum. The lipid peroxidation ratio (cortex/striatum) was found to increase significantly ($P < 0.05$) by 59.6% in the cytosol, while the mitochondria showed only 29.3% increase by the end of 24-h reperfusion compared to sham. On the other hand, the endogenous non-enzymatic antioxidant GSH ratio (cortex/striatum) increased significantly ($P < 0.05$) by 46.6% in cytosol alone at the end of 24-h reperfusion. GSH
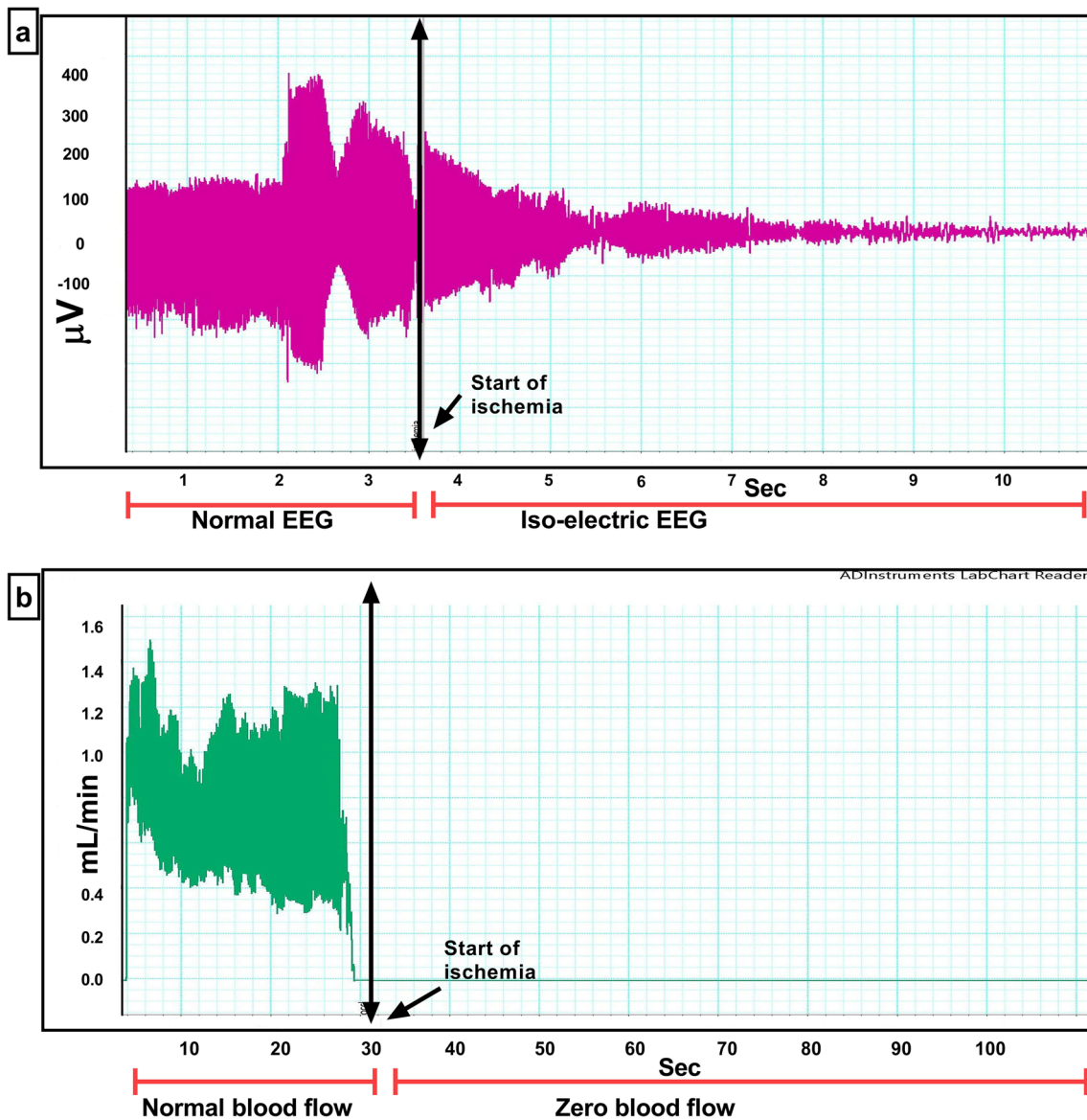
Fig. 1 Induction of ischemia-reperfusion injury. The induction of ischemia was confirmed by **a** the isoelectric pattern of EEG and **b** zero flow indication of flow meter probe

ratio in mitochondria elevated significantly ($P < 0.05$) at 15 min ischemia (78.2%) and 30 min reperfusion (49.3%) but reduced by 31.1% by end of 24 h reperfusion compared to sham.

Hence, based on results from Table 1, it was clear that mitochondria lipid peroxidation levels and GSH levels were normalized by 24 h reperfusion compared to sham despite having significant variations at earlier time points. As a further step to probe the significant alterations in the cytosol, we assessed the antioxidant enzymes and the data is presented in Table 2. More prominently, we found that SOD activity showed significant ($P < 0.05$) increase from sham at 24 h reperfusion in the striatum alone. Hence, the SOD ratio showed a significant ($P < 0.05$) decline of 44.4% by 24 h compared to sham. Catalase activity from these regions showed significant

($P < 0.05$) increase at initial times of ischemia and reperfusion but subsequently went down by the end of 24 h compared to sham. The catalase ratio reduced significantly ($P < 0.05$) by 57.8% at the end of 4 h and the recovered by 24 h compared to sham. Hence, it was evident that the antioxidant enzyme variations causing oxidative stress were significant compared to sham but occurred in a phased manner across the time points. The GPx and GR activities in cortex had no significant variation and hence, this balance maintained the GSH level in cortex close to the sham. On the other hand, a reduction of 14.3% in the GR activity in striatum reduced its GSH content, while the GPx activity was close to sham level (Table 2).

To verify the significantly elevated SOD activity ratio at the end of 4- to 24-h reperfusion, which was due to its increased activity in the striatum, we assessed the gene expression for the
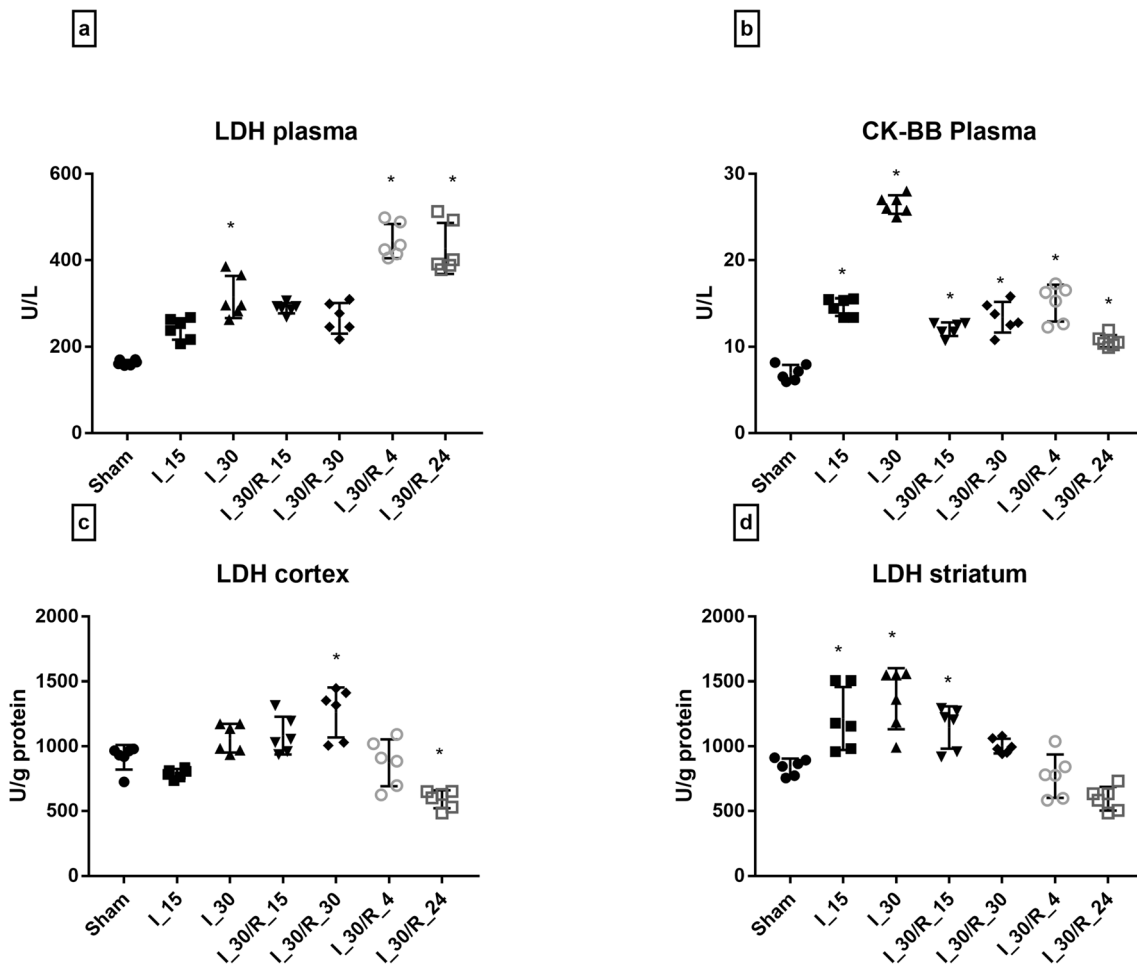
Fig. 2 Injury marker assessment. The extent of injury produced by brain IRI was quantified from the biochemical activity of **a** LDH in plasma, **b** CK-BB in plasma, **c** LDH in cortex, and **d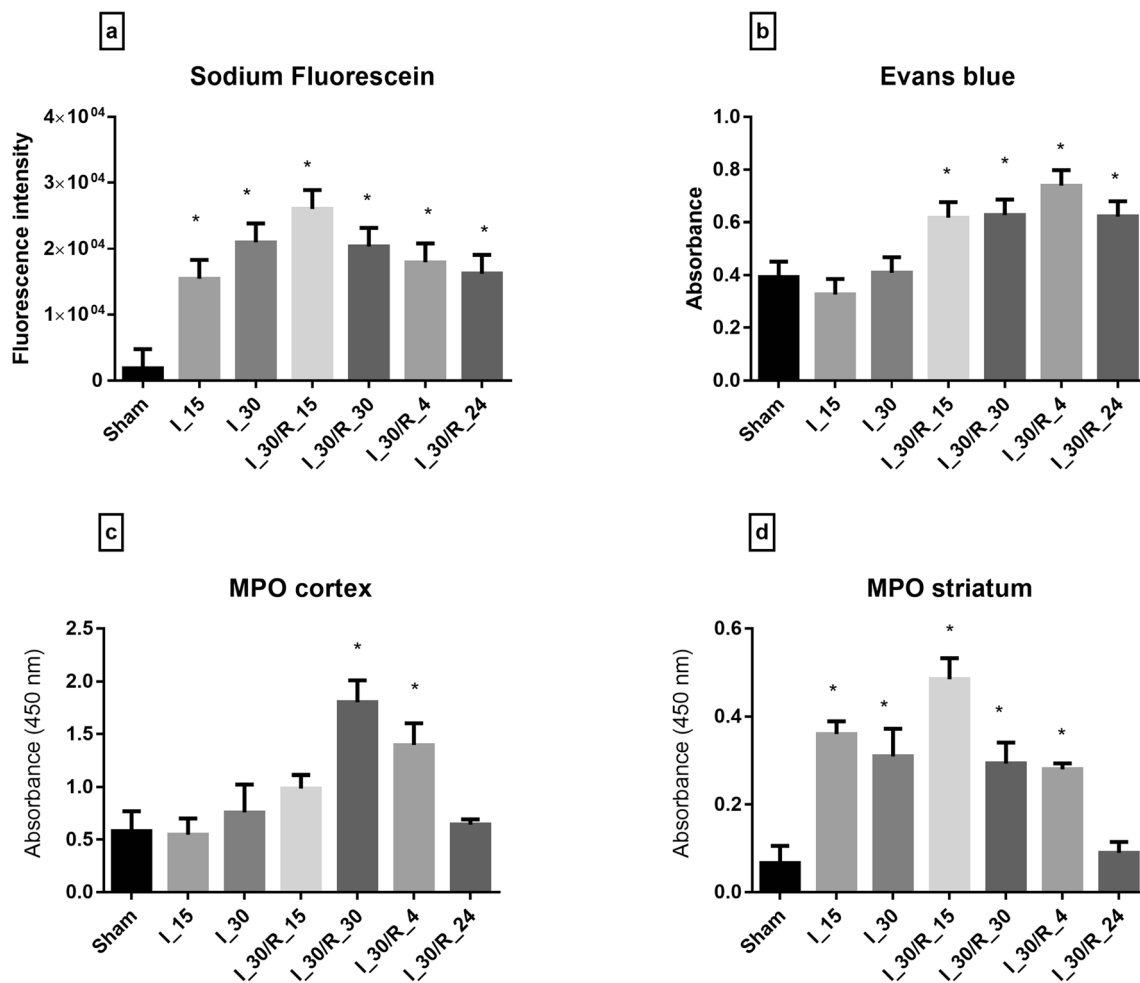** LDH in the striatum. The data are presented as mean ± SEM of 6 independent observations per group. *$P < 0.05$ vs sham

two isoforms of SOD, namely, CuZn-SOD and Mn-SOD across the two brain regions: cortex and striatum (Fig. 5a, b). From Fig. 5, consistent with the observations of enzyme activity, Mn-SOD was overexpressed significantly ($P < 0.05$) by > 9 fold at the end of 24-h reperfusion in striatum alone (Fig. 5b).

Based on the above results, to assess the intactness of mitochondrial function, we measured the levels of cellular energy fuel ATP in the brain regions wherein the striatum (Fig. 5d) showed immediate and higher sensitivity to variation in ATP compared to cortex (Fig. 5c). In the striatum, ATP declined

Fig. 3 Apoptosis in the brain regions affected by IRI. The apoptosis induced due to brain IRI is presented by the activity of caspase-3 from the two brain region **a** cortex and **b** striatum. The data are presented as mean ± SEM of 6 independent observations per group. *$P < 0.05$ vs sham
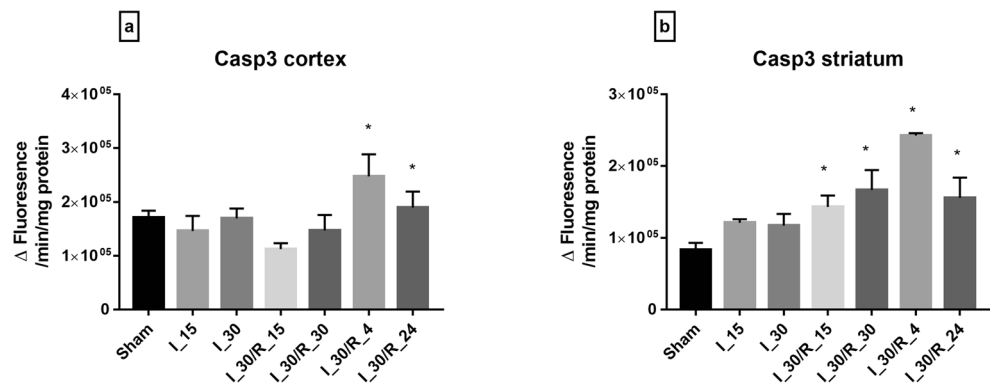
Fig. 4 Disruption of BBB and inflammatory activity in the brain. The main feature of brain IRI is the disruption of the blood-brain barrier and entry of leukocytes leading to vascular inflammatory activity. The BBB leakage was measured from the extravasation of **a** sodium fluorescein and **b** Evans blue. The inflammation was measured by the activity of myeloperoxidase in **c** cortex and **d** striatum. The data are presented as mean ± SEM of 6 independent observations per group. *$P < 0.05$ vs sham

significantly ($P < 0.05$) by 30-min ischemia and at 4-h reperfusion, while cortex had significantly ($P < 0.05$) low ATP level at 24 h alone.

Impact of ischemia-reperfusion injury on the cognitive performance in the rat

Though injury, inflammation, and apoptosis partially normalized, we noted that higher lipid peroxidation persisted in the cortical region. As memory deficits occur due to oxidative stress in the prefrontal cortex and hippocampus in cerebral IRI model, we observed the behavioral performance of rat in the radial arm maze and Morris water maze (Online Resource 1) (Gehring et al. 2015). From Fig. 6, before ischemia, the WMI was > 2.5 for all the rats, which started to decline post reperfusion to a value of 1 or 0 by the end of 5 days after IRI (Fig. 6a). The correct choices made for pellet retrieval also showed a similar trend (Fig. 6b). In the water maze, the time taken and distance traveled to reach platform took longer in

ischemia-induced rats, more significantly in the 30 min group (Fig. 6c, d) than the 15-min ischemic rats. In the water maze test, significant ($P < 0.05$) difference in performance of rats was noted even among I15 and I30.

Discussion

The present study focused on biochemical alterations, injury, and oxidative stress in the brain and its regions, arising due to ischemia and reperfusion injury at various time intervals in rat brain. The results suggested an imminent entry of low molecular weight proteins due to disruption in BBB permeability during 15 to 30 min of ischemia. Reperfusion following 30 min of ischemia further enhanced the BBB permeability to high molecular weight proteins that subsided by 24 h along with the inflammatory activity. TTC staining was considered to evaluate the infarct produced, but the limitation of its effectiveness in short duration has precluded its use. However the

Table 1 Lipid peroxidation and GSH level in the brain regions and their mitochondria

Groups	Cortex	Striatum	mt-Cortex	mt-Striatum	Ratio Cortex/striatum	Ratio mt- cortex/ mt- striatum
TBARS (nM MDA/g)						
Sham	0.17 ± 0.01	0.09 ± 0.02	2.2 ± 0.46	1.4 ± 0.11	1.83 ± 0.32	1.22 ± 0.14
I_15	$0.42 \pm 0.03^*$	$0.31 \pm 0.03^*$	2.4 ± 0.41	2.9 ± 0.05	1.35 ± 0.33	0.83 ± 0.19
I_30	$0.45 \pm 0.05^*$	$0.32 \pm 0.04^*$	2.8 ± 0.67	$3.3 \pm 0.16^*$	1.15 ± 0.28	0.85 ± 0.09
I_30/R_15	$0.48 \pm 0.06^*$	$0.27 \pm 0.04^*$	2.5 ± 0.54	2.7 ± 0.16	1.77 ± 0.4	0.93 ± 0.15
I_30/R_30	$0.37 \pm 0.02^*$	0.15 ± 0.04	$4.7 \pm 0.63^*$	2.6 ± 0.21	2.46 ± 0.35	$1.81 \pm 0.12^*$
I_30/R_4	0.28 ± 0.04	0.01 ± 0.01	3.0 ± 0.26	1.7 ± 0.19	$2.82 \pm 0.29^*$	1.76 ± 0.14
I_30/R_24	$0.68 \pm 0.04^*$	0.15 ± 0.01	2.6 ± 0.20	1.5 ± 0.02	$4.53 \pm 0.35^*$	1.73 ± 0.15
GSH (mg/mg protein)						
Sham	0.027 ± 0.006	0.031 ± 0.004	0.020 ± 0.003	0.027 ± 0.003	0.87 ± 0.15	0.74 ± 0.29
I_15	0.033 ± 0.002	0.037 ± 0.004	0.016 ± 0.001	$0.005 \pm 0.002^*$	0.89 ± 0.14	$3.40 \pm 0.30^*$
I_30	0.034 ± 0.003	$0.054 \pm 0.006^*$	0.016 ± 0.004	$0.014 \pm 0.002^*$	0.63 ± 0.13	1.14 ± 0.26
I_30/R_15	0.037 ± 0.002	0.043 ± 0.005	0.016 ± 0.002	0.018 ± 0.001	0.86 ± 0.11	0.89 ± 0.22
I_30/R_30	$0.048 \pm 0.002^*$	0.040 ± 0.003	0.019 ± 0.001	$0.013 \pm 0.002^*$	1.20 ± 0.13	$1.46 \pm 0.27^*$
I_30/R_4	0.036 ± 0.001	0.020 ± 0.002	0.016 ± 0.003	0.034 ± 0.001	$1.80 \pm 0.11^*$	0.47 ± 0.30
I_30/R_24	0.031 ± 0.001	$0.019 \pm 0.002^*$	0.018 ± 0.001	0.035 ± 0.002	$1.63 \pm 0.15^*$	0.51 ± 0.27

The oxidative stress generated by brain IRI was measured in the cytosol and mitochondria from the amount of malondialdehyde formed using the TBARS assay and the levels of endogenous antioxidant reduced glutathione (GSH), from the two brain regions cortex and striatum. The data are presented as mean ± SEM of 6 independent observations per group. *$P < 0.05$ vs sham, *mt* mitochondria

area at risk was measured at various ischemic and reperfusion time points (Online resource 1), which was maximum at 30 min of reperfusion and reduced by 24 h, correlating with changes in the BBB disruption. Biochemical assessment from CK-BB and caspase-3 suggested a similar trend of progressive recovery by 24 of reperfusion. However, we found that oxidative stress at the cellular level was not normalized as lipid peroxidation within the brain continued to remain elevated

Table 2 Antioxidant enzyme activities across brain regions

Groups	Cortex	Striatum	Ratio	Cortex	Striatum	Ratio
	SOD (U/mg protein)			Catalase (U/mg protein)		
Sham	0.35 ± 0.02	0.56 ± 0.01	0.63 ± 0.10	0.51 ± 0.01	0.50 ± 0.05	1.02 ± 0.15
I_15	0.29 ± 0.03	0.53 ± 0.02	0.55 ± 0.05	0.55 ± 0.07	0.84 ± 0.01	0.65 ± 0.11
I_30	$0.27 \pm 0.01^*$	0.50 ± 0.04	0.54 ± 0.04	0.76 ± 0.06	$0.86 \pm 0.06^*$	0.88 ± 0.09
I_30/R_15	$0.28 \pm 0.01^*$	0.48 ± 0.01	0.58 ± 0.08	$1.00 \pm 0.10^*$	$0.86 \pm 0.09^*$	1.16 ± 0.13
I_30/R_30	0.38 ± 0.01	$0.45 \pm 0.02^*$	0.84 ± 0.09	$1.00 \pm 0.10^*$	0.62 ± 0.05	1.61 ± 0.11
I_30/R_4	0.37 ± 0.01	$0.31 \pm 0.01^*$	$1.19 \pm 0.10^*$	0.27 ± 0.05	0.63 ± 0.07	$0.43 \pm 0.09^*$
I_30/R_24	$0.24 \pm 0.06^*$	$0.68 \pm 0.01^*$	$0.35 \pm 0.10^*$	0.41 ± 0.07	0.35 ± 0.02	1.17 ± 0.08
	GPx (mg GSH/mg protein)			GR (μM NADPH oxidized/min/mg protein)		
Sham	1.022 ± 0.05	1.256 ± 0.01	0.81 ± 0.02	8925 ± 923	6270 ± 614	1.42 ± 0.19
I_15	1.111 ± 0.08	1.216 ± 0.02	0.91 ± 0.05	7670 ± 334	8511 ± 868	0.90 ± 0.11
I_30	1.093 ± 0.08	$1.191 \pm 0.01^*$	0.92 ± 0.03	9062 ± 249	$12,031 \pm 134^*$	0.75 ± 0.15
I_30/R_15	0.987 ± 0.04	$1.158 \pm 0.01^*$	0.85 ± 0.02	9143 ± 439	$10,750 \pm 125$	0.85 ± 0.09
I_30/R_30	1.145 ± 0.07	$1.161 \pm 0.02^*$	0.99 ± 0.02	$1331 \pm 714^*$	8959 ± 109	$0.15 \pm 0.12^*$
I_30/R_4	1.142 ± 0.01	1.228 ± 0.01	0.93 ± 0.03	9486 ± 342	5419 ± 101	1.75 ± 0.16
I_30/R_24	1.135 ± 0.02	1.246 ± 0.02	0.91 ± 0.02	5972 ± 331	$5371 \pm 401^*$	1.11 ± 0.15

The oxidative stress generated by brain IRI was measured from the activities of antioxidant enzymes from two brain regions cortex and striatum for superoxide dismutase-SOD, catalase, glutathione peroxidase (GPx), and glutathione reductase (GR). The data are presented as mean ± SEM of 6 independent observations per group. *$P < 0.05$ vs sham

even at 24 h of reperfusion, which is often overlooked in most reported investigations. Upon examining this stress, we found it to be varying even among the two brain regions, i.e., cortex and striatum. These stress differences extended even to the mitochondria and contributed to an overall decline in the cognitive performance of rat. The difference in antioxidant systems within the cytosol and organelle is thought to be the major reason behind the cellular stress despite normalization of overall injury.

An acute occlusion of cerebral arteries that leads to cell death in the territory of ischemic tissue is associated with stroke episodes, traumatic head injury, carotid endarterectomy, aneurysm repair, or deep hypothermic circulatory arrest. Animal studies in the past could not provide a holistic view on cerebral IRI compiling all the aspects of injury histology, blood-brain barrier damage, molecular mechanisms, and regional variations in a single model (Candelario-Jalil et al. 2001; Ordy et al. 1993; Selakovic et al. 2011). Similar preceding studies used gerbil as a model, whose cerebral vascular anatomy varies from that of the rat. As most of the present preclinical trial data on therapeutics are generated from rat as a preferred model for IRI (PubMed: 5120 in rat against 401 in gerbils), it is necessary to map the changes in rat brain within the 24 h of reperfusion following cerebral ischemia. In addition, as oxidative stress is well-characterized phenomenon contributing to apoptosis during cerebral IRI, significant information on this stress experienced during ischemia and reperfusion with respect to the brain regions is obscure. The clamping of right and left carotid arteries for a stipulated time was done to establish ischemia, which was confirmed by isoelectric EEG and zero real-time flow rate, followed by removal of the clamp to establish the perfusion (Fig. 1). In the present model, although the carotid arteries are occluded, limited amount of blood supply to the brain is maintained via the vertebral arteries connected to the circle of Willis. Even though this model may not produce extensive area of infarct within 30 min of ischemia (Raval et al. 2009), it is sufficient to induce various pathological reactions associated with reperfusion injury that may lead to the BBB disruption (Chen et al. 2009). Yen and colleagues demonstrated that the entry and distribution of low (< 300 Da) and high molecular weight proteins (> 400 Da) through the BBB varies across the regions and can be detected using tracer dyes NaF and EB. Using this approach, in the present study, we observed the entry of low molecular weight proteins during ischemia and high molecular weight ones during reperfusion (Yen et al. 2013). Interestingly, in the present study, by the end of 24 h, the high molecular weight protein entry declined and was limited to lower ones only (Fig. 4). This observation of ours was in agreement with a previous study wherein stroke induced a biphasic change

in BBB disruption that is partially reversible over time (Chen et al. 2014). In the present study, these observations were in accordance with the CK-BB levels in plasma that increased steadily over a time course of 30 min of reperfusion and partially reduced by 24-h reperfusion (Fig. 2). In addition, neutrophil infiltration, a characteristic feature of IRI, was measured from the MPO activity and followed a similar pattern of reversal to near normal levels by the end of 24-h reperfusion in the brain parenchyma (Fig. 4). This acute phase inflammatory responses (TNF-α, IL-6, and IL-8) during IRI are well documented to trigger apoptosis via FHL2 protein (Anselmi et al. 2004). In the present study, we observed caspase-3 activity to be significantly elevated in the brain by 24 h despite a reversal of BBB leakage, inflammation, and reduction of area at risk. Apoptosis, being an active ATP-dependent process (Anselmi et al. 2004), we observed a reduced ATP level in the brain at the 24 h of reperfusion which was in support of our current findings (Fig. 5).

The fact that permeability of BBB varies with respect to regions of the brain (Yen et al. 2013), especially hippocampal CA1 and DG being highly vulnerable to ischemic insults prompted us to probe the biochemical changes regionally. Prominently, we noted these changes in two regions of brain, i.e., cortex and striatum (comprising of the hippocampus). It was observed clearly that inflammatory activity raised significantly with 15 min of ischemia alone in the striatum and also had an elevated LDH activity in this region (Fig. 2). The corresponding caspase-3 activity showed significant elevation ($P < 0.05$) from 15 min of reperfusion and remained higher even at 24 h (Fig. 3). However, unlike the cortex, the higher apoptotic activity did not coincide with the ATP level in the striatum that remained at normal levels after 24-h reperfusion. This may be due to differences in activation of caspase-3 by either intrinsic or extrinsic pathway (Mak and Yeh 2002). Hence, we assessed the oxidative stress experienced by the two regions at the cellular level. Similar studies in the past have shown that maximum oxidative damage was produced in gerbil brain that has a highly variable circle of Willis that is often incomplete. The damage persisted even after 28 days after reperfusion (Candelario-Jalil et al. 2001; Selakovic et al. 2011). This emphasizes the need to probe the oxidative stress at the cellular and regional levels that may cause adversities at later stages.

Oxidative stress experienced by the brain tissue decides whether the ischemic region could be salvaged by reperfusion procedures or pharmacological interventions. Studies have indicated that functional restoration of cells in ischemic core and peri-infarct regions were observed when oxidative stress is reversed (Bulteau et al. 2004). In the present study, we noted that the lipid peroxidation
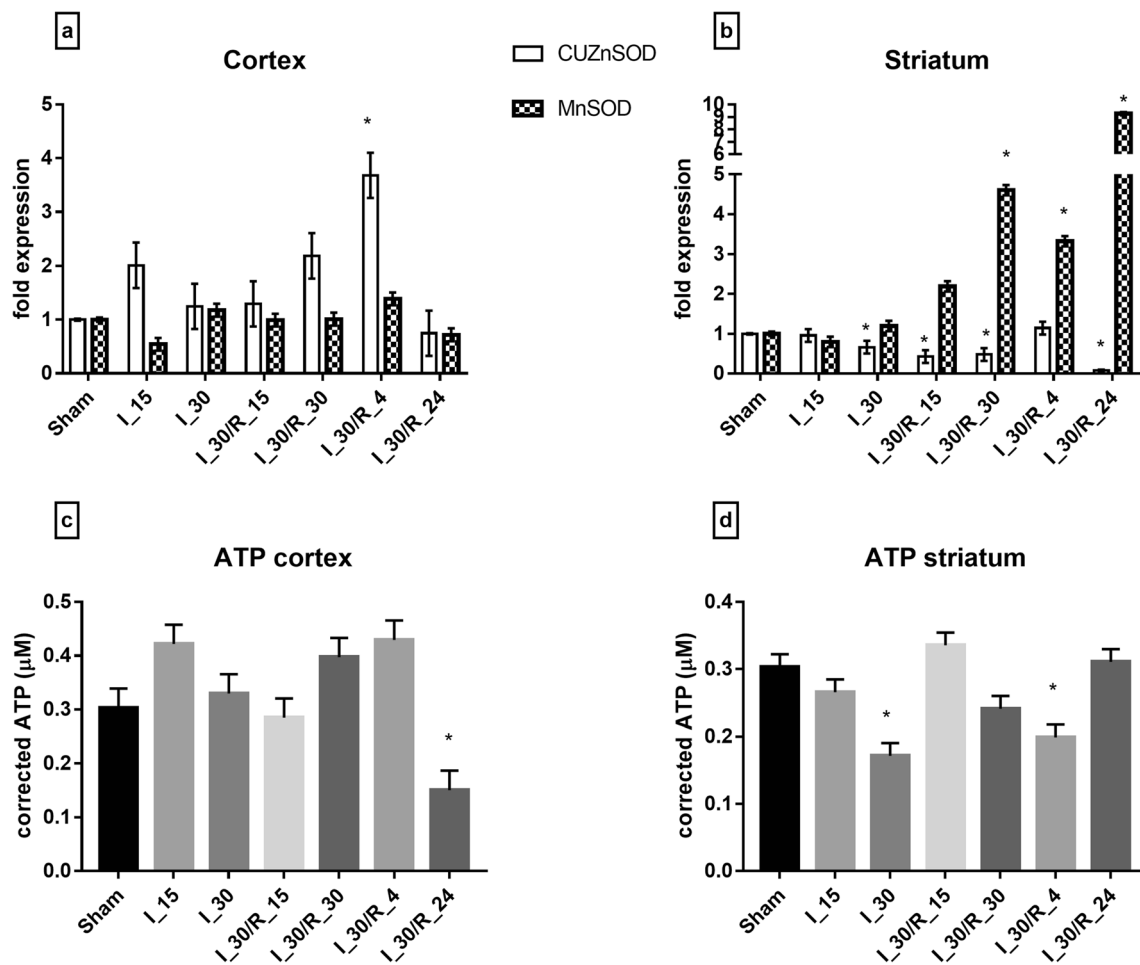
Fig. 5 Gene expression analysis. The gene expressions of a Cu–Zn SOD and b Mn-SOD were analyzed at various time points of ischemia and reperfusion along with the extent of ATP generated in c cortex and d striatum. The data are presented as mean ± SEM of 6 independent observations per group. $*P < 0.05$ vs sham

ratio (cortex/striatum) increased in a time-dependent manner from 30 min of reperfusion, with 24 h showing a significantly ($P < 0.05$) higher ratio in the cytosolic fraction (Table 1). To assess if the subcellular component, i.e., mitochondria, also had a similar trend, we assessed the mitochondrial fractions from the two regions and found the lipid peroxidation ratio was higher at 24 h. On the contrary, the cellular non-enzymatic antioxidant GSH ratio (cortex/striatum) declined in mitochondria alone but not in the cytosol. As glutathione production is tightly regulated by the activities of enzymatic antioxidant system (SOD, Catalase, GPx, and GR), we assessed their ratio (cortex/striatum) and found that a balance between GPx and GR was established (ratio close to 1- GR > GPx) by the end of 24 h of reperfusion and hence the ratio of GSH in cytosol across the brain regions remained higher despite higher lipid peroxidation stress (Table 2). On the other hand, as oxidative stress is known to deplete antioxidant enzyme activities in the current model (Homi et al. 2002), we observed reduced catalase activity ratio

in the initial times of ischemia and reperfusion owing to reduced cortical activity but returned close to normal by the end of 24 h. However, the SOD activity in cytosol was significantly elevated at 24 h in striatum despite having lower lipid peroxidation and therefore, a decline in the ratio was noted at this time point (Fig. 5). A similar study done on gerbils using a 5-min occlusion model demonstrated that the oxidative damage was higher in the hippocampus until 96 h of reperfusion (Candelario-Jalil et al. 2001). As Gerbils have an anatomical variation in the circle of Willis supplying the brain regions compared to a rat, it is interesting to observe that striatum recovered from oxidative damage in the rat, which was not the case in gerbils. However, the same study reported Mn-SOD to be higher in the hippocampus at 72 h of reperfusion after 5 min of ischemia. To probe the unusual rise in SOD activity in this region, we assessed the expression of SOD mRNA for two of its isozymes Mn-SOD and Cu/ Zn-SOD across the cortex and striatum. We found Mn-SOD to be significantly overexpressed with time (> 9
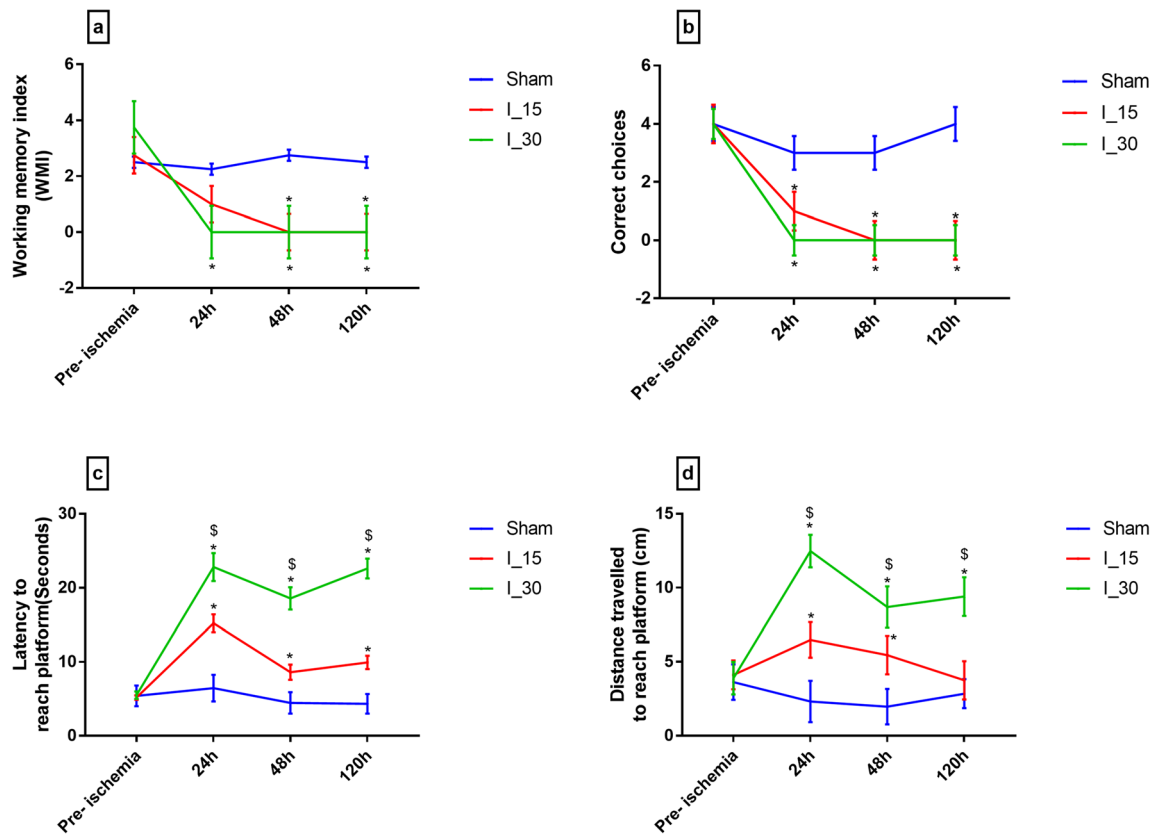
Fig. 6 Cognitive assessment in rat subjected to IRI. The cognitive assessment of rat on radial arm maze and Morris water maze was performed and reported before ischemia and 24, 48, and 120 h after reperfusion following 30-min ischemia, as **a** working memory index (WMI), **b** correct choices made, **c** latency to reach the platform, and **d** distance traveled to reach the platform. The data are presented as mean ± SEM of 6 independent observations per group. *$P < 0.05$ vs sham, $^{\$}P < 0.5$ I15 vs I30

fold) in the striatum by 24 h of reperfusion (Fig. 5b). This answers why the oxidative stress linked ATP decline was not observed in the striatum at 24 h of reperfusion, despite its reduction in the cortex. This also explains the importance of regional oxidative stress that declined in the striatum by 24 h of reperfusion while not in the cortex.

Conclusion

Overall, this study followed the events of ischemia-reperfusion on injury, apoptosis, and oxidative stress in rat brain regions and found that despite alleviation of the former, oxidative damage persisted at the cellular level. However, its
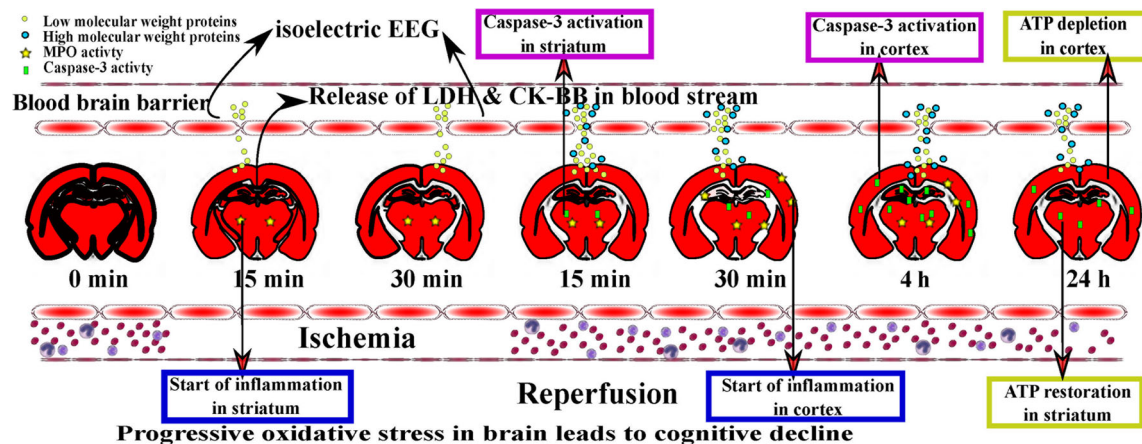
Fig. 7 The pathological and biochemical changes occurring in the rat brain subjected to ischemia-reperfusion injury is presented on a timeline of events occurring during ischemia (15 and 30 min) and reperfusion (15 min, 30 min, 4 h, and 24 h). The regional variations in biochemical alterations are presented for cortex and striatum in terms of inflammation, apoptosis, and ATP level. The changes in BBB dysfunction and area at risk are presented at all time points to clearly understand the pathology

impact, in the long run, can be judged conspicuously from the functional outcome in these models by assessing the memory disturbances and cognitive deficits. A similar study has demonstrated that cerebral ischemia-associated oxidative stress affects the prefrontal cortex and hippocampus that results in cognitive defects without loss in locomotor or exploratory activity (Schaar et al. 2010; Schimidt et al. 2014). Hence, in the present study, the radial arm maze and water maze performance in the rats were assessed after 15 min and 30 min of ischemia followed by reperfusion and found that cognitive ability declined in both cases and could not recover even after 5 days of testing. The observations of the present study are represented in the graphical abstract (Fig. 7) for a holistic view. Further studies may be required to evaluate the selective subcellular stress in these regions as our previous studies suggest distinct sensitivity of mitochondria (interfibrillar and subsarcolemmal mitochondria) to ischemia-reperfusion associated stress in the heart (Banu et al. 2016).

Author contributions Gino Kurian designed the study and interpreted the data. Sriram Ravindran conducted the surgery, behavioral studies, biochemical experiments, and statistical analysis. Both the authors were involved in writing and thorough review of the manuscript.

Compliance with ethical standards

Conflict of interest The authors declare that they have no conflicts of interest

References

Almeida A, Allen KL, Bates TE, Clark JB (1995) Effect of reperfusion following cerebral ischaemia on the activity of the mitochondrial respiratory chain in the gerbil brain. J Neurochem 65: 1698–1703

Anselmi A, Abbate A, Girola F, Nasso G, Biondi-Zoccai GG, Possati G, Gaudino M (2004) Myocardial ischemia, stunning, inflammation, and apoptosis during cardiac surgery: A review of evidence. Eur J Cardiothorac Surg 25:304–311. https://doi.org/10.1016/j.ejcts.2003. 12.003

Bačić G, Pavićević A, Peyrot F (2016) In vivo evaluation of different alterations of redox status by studying pharmacokinetics of nitroxides using magnetic resonance techniques. Redox Biol 8: 226–242. https://doi.org/10.1016/j.redox.2015.10.007

Bai J, Lyden PD (2015) Revisiting cerebral postischemic reperfusion injury: New insights in understanding reperfusion failure, hemorrhage, and edema. Int J Stroke 10:143–152. https://doi.org/10. 1111/ijs.12434

Banu SA, Ravindran S, Kurian GA (2016) Hydrogen sulfide postconditioning preserves interfibrillar mitochondria of rat heart during ischemia reperfusion injury. Cell Stress Chaperones 21:571–582. https://doi.org/10.1007/s12192-016-0682-8

Baron J-C, Yamauchi H, Fujioka M, Endres M (2013) Selective neuronal loss in ischemic stroke and cerebrovascular disease. J Cereb Blood Flow Metab 34:2–18. https://doi.org/10.1038/jcbfm.2013.188

Barrientos A, Fontanesi F, Díaz F (2009) Evaluation of the mitochondrial respiratory chain and oxidative phosphorylation system using polarography and spectrophotometric enzyme assays. Current protocols in human genetics / editorial board, Jonathan L. Haines … [et al.] CHAPTER:Unit19.3-Unit19.3. https://doi.org/10.1002/ 0471142905.hg1903s63

Bruin JP de, Sanchez-Santed F, Heinsbroek RP, Donker A, Postmes P (1994) A behavioural analysis of rats with damage to the medial prefrontal cortex using the Morris water maze: evidence for behavioural flexibility, but not for impaired spatial navigation. Brain Res 652:323–333

Brustovetsky N, Brustovetsky T, Purl KJ, Capano M, Crompton M, Dubinsky JM (2003) Increased susceptibility of striatal mitochondria to calcium-induced permeability transition. J Neurosci 23: 4858–4867

Bulteau A-L, Lundberg KC, Ikeda-Saito M, Isaya G, Szweda LI (2004) Reversible redox-dependent modulation of mitochondrial aconitase and proteolytic activity during in vivo cardiac ischemia/reperfusion. Proc Natl Acad Sci U S A 102:5987–5991. https://doi.org/10.1073/ pnas.0501519102

Candelario-Jalil E, Mhadu NH, Al-Dalain SM, Martinez G, Leon OS (2001) Time course of oxidative damage in different brain regions following transient cerebral ischemia in gerbils. Neurosci Res 41: 233–241

Chen B, Friedman B, Cheng Q, Tsai P, Schim E, Kleinfeld D, Lyden PD (2009) Severe Blood–Brain Barrier Disruption and Surrounding Tissue Injury. Stroke 40:e666. https://doi.org/10.1161/ STROKEAHA.109.551341

Chen W, Sun Y, Liu K, Sun X (2014) Autophagy: a double-edged sword for neuronal survival after cerebral ischemia. Neural Regen Res 9: 1210–1216. https://doi.org/10.4103/1673-5374.135329

Chinopoulos C, Zhang SF, Thomas B, Ten V, Starkov AA (2011) Isolation and functional assessment of mitochondria from small amounts of mouse brain tissue. Methods Mol Biol 793:311–324. https://doi.org/10.1007/978-1-61779-328-8_20

Davis M, Whitely T, Turnbull DM, Mendelow AD (1997) Selective impairments of mitochondrial respiratory chain activity during aging and ischemic brain damage. Acta Neurochir Suppl 70:56–58

Erecińska M, Silver IA (2001) Tissue oxygen tension and brain sensitivity to hypoxia. Respir Physiol 128:263–276. https://doi.org/10. 1016/S0034-5687(01)00306-1

Fontaine E, Eriksson O, Ichas F, Bernardi P (1998) Regulation of THE permeability transition pore in skeletal muscle mitochondria: modulation by electron flow through the respiratory chain complex I. J Biol Chem 273:12662–12668. https://doi.org/10.1074/jbc.273.20. 12662

Friberg H, Connern C, Halestrap AP, Wieloch T (1999) Differences in the activation of the mitochondrial permeability transition among brain regions in the rat correlate with selective vulnerability. J Neurochem 72:2488–2497

Friberg H, Wieloch T, Castilho RF (2002) Mitochondrial oxidative stress after global brain ischemia in rats. Neurosci Lett 334:111–114

Garbarino VR, Orr ME, Rodriguez KA, Buffenstein R (2015) Mechanisms of Oxidative Stress Resistance in The Brain: Lessons Learned From Hypoxia Tolerant Extremophilic Vertebrates. Arch Biochem Biophys 576:8–16. https://doi.org/10.1016/j.abb.2015.01. 029

Gehring TV, Luksys G, Sandi C, Vasilaki E (2015) Detailed classification of swimming paths in the Morris water maze: multiple strategies within one trial. Sci Rep 5:14562. https://doi.org/10.1038/srep14562

Gilbert K, Godbout R, Rousseau G (2016) Caspase-3 Activity in the Rat Amygdala Measured by Spectrofluorometry After Myocardial Infarction. J Vis Exp 53207. https://doi.org/10.3791/53207

Eventual analysis of global cerebral ischemia-reperfusion injury in rat brain: a paradigm of a shift in...

593

Granger DN, Kvietys PR (2015) Reperfusion injury and reactive oxygen species: the evolution of a concept. Redox Biol 6:524–551. https://doi.org/10.1016/j.redox.2015.08.020

Hebert-Chatelain E, Desprez T, Serrat R, Bellocchio L, Soria-Gomez E, Busquets-Garcia A, Pagano Zottola AC, Delamarre A, Cannich A, Vincent P, Varilh M, Robin LM, Terral G, García-Fernández MD, Colavita M, Mazier W, Drago F, Puente N, Reguero L, Elezgarai I, Dupuy J-W, Cota D, Lopez-Rodriguez M-L, Barreda-Gómez G, Massa F, Grandes P, Bénard G, Marsicano G (2016) A cannabinoid link between mitochondria and memory. Nature 539:555 EP–555559. https://doi.org/10.1038/nature20127

Homi HM, Freitas JJS, Curi R, Velasco IT, Junior BAS (2002) Changes in superoxide dismutase and catalase activities of rat brain regions during early global transient ischemia/reperfusion. Neurosci Lett 333:37–40

Hu Y, Deng H, Xu S, Zhang J (2015) MicroRNAs regulate mitochondrial function in cerebral ischemia-reperfusion injury. Int J Mol Sci 16:24895–24917. https://doi.org/10.3390/ijms161024895

Jonas EA, Mnatsakanyan N, Miranda P, Park H-A, Chen R, Licznerski P, Weinert M, Smith PJ, Chavez A, Zukin RS, Gribkoff VK, Alavian KN (2017) Mitochondria and memory: bioenergetics, synaptic plasticity and neurodegeneration. Biophys J 112:180a. https://doi.org/10.1016/j.bpj.2016.11.996

Kahl A, Stepanova A, Konrad C, Anderson C, Manfredi G, Zhou P, Iadecola C, Galkin A (2018) Critical role of flavin and glutathione in complex I-mediated bioenergetic failure in brain ischemia/reperfusion injury. Stroke 49:1223–1231. https://doi.org/10.1161/STROKEAHA.117.019687

Kalogeris T, Baines CP, Krenz M, Korthuis RJ (2012) Cell Biology of Ischemia/Reperfusion Injury. Int Rev Cell Mol Biol 298:229–317. https://doi.org/10.1016/B978-0-12-394309-5.00006-7

Kobayashi T, Kuroda S, Tada M, Houkin K, Iwasaki Y, Abe H (2003) Calcium-induced mitochondrial swelling and cytochrome c release in the brain: its biochemical characteristics and implication in ischemic neuronal injury. Brain Res 960:62–70

Kumar R, Bukowski MJ, Wider JM, Reynolds CA, Calo L, Lepore B, Tousignant R, Jones M, Przyklenk K, Sanderson TH (2016) Mitochondrial dynamics following global cerebral ischemia. Mol Cell Neurosci 76:68–75. https://doi.org/10.1016/j.mcn.2016.08.010

Kumari Naga K, Panigrahi M, Prakash Babu P (2007) Changes in endogenous antioxidant enzymes during cerebral ischemia and reperfusion. Neurol Res 29:877–883. https://doi.org/10.1179/016164107X181842

Lai JC, Walsh JM, Dennis SC, Clark JB (1977) Synaptic and non-synaptic mitochondria from rat brain: isolation and characterization. J Neurochem 28:625–631

Lee J-M, Grabb MC, Zipfel GJ, Choi DW (2000) Brain tissue responses to ischemia. J Clin Invest 106:723–731

Li Y, Schellhorn HE (2007) Rapid kinetic microassay for catalase activity. J Biomol Tech 18:185–187

Li P-A, Liu G-J, He QP, Floyd RA, Siesjö BK (1999) Production of hydroxyl free radical by brain tissues in hyperglycemic rats subjected to transient forebrain ischemia. Free Radic Biol Med 27:1033–1040. https://doi.org/10.1016/S0891-5849(99)00152-5

Lim CC, Bryan NS, Jain M, Garcia-Saura MF, Fernandez BO, Sawyer DB, Handy DE, Loscalzo J, Feelisch M, Liao R (2009) Glutathione peroxidase deficiency exacerbates ischemia-reperfusion injury in male but not female myocardium: insights into antioxidant compensatory mechanisms. Am J Physiol Heart Circ Physiol 297:H2144–H2153. https://doi.org/10.1152/ajpheart.00673.2009

Liu F, Lu J, Manaenko A, Tang J, Hu Q (2018) Mitochondria in ischemic stroke: new insight and implications. Aging Dis 9:924–937. https://doi.org/10.14336/AD.2017.1126

Lunnon K, Keohane A, Pidsley R, Newhouse S, Riddoch-Contreras J, Thubron EB, Devall M, Soininen H, Kloszewska I, Mecocci P, Tsolaki M, Vellas B, Schalkwyk L, Dobson R, Malik AN, Powell J, Lovestone S, Hodges A (2017) Mitochondrial genes are altered in blood early in Alzheimer's disease. Neurobiol Aging 53:36–47. https://doi.org/10.1016/j.neurobiolaging.2016.12.029

Mak TW, Yeh W-C (2002) Signaling for survival and apoptosis in the immune system. Arthritis Res 4(Suppl 3):S243–S252. https://doi.org/10.1186/ar569

Margaritescu O, Mogoanta L, Pirici I, Pirici D, Cernea D, Margaritescu C (2009) Histopathological changes in acute ischemic stroke. Romanian J Morphol Embryol 50:327–339

Martin LJ (2012) Biology of mitochondria in neurodegenerative diseases. Prog Mol Biol Transl Sci 107:355–415. https://doi.org/10.1016/B978-0-12-385883-2.00005-9

Martins IVA, Rivers-Auty J, Allan SM, Lawrence CB (2017) Mitochondrial abnormalities and synaptic loss underlie memory deficits seen in mouse models of obesity and Alzheimer's disease. J Alzheimers Dis 55:915–932. https://doi.org/10.3233/JAD-160640

Matire H, Harry M, Kathryn M, Mark W (2000) Ethnicity and equity: missing the point. Stroke 31:2517–2527. https://doi.org/10.1161/01.STR.31.10.2517

Nandi A, Chatterjee IB (1988) Assay of superoxide dismutase activity in animal tissues. J Biosci 13:305–315. https://doi.org/10.1007/BF02712155

Nishizawa Y (2001) Glutamate release and neuronal damage in ischemia. Life Sci 69:369–381

Ohkawa H, Ohishi N, Yagi K (1979) Assay for lipid peroxides in animal tissues by thiobarbituric acid reaction. Anal Biochem 95:351–358. https://doi.org/10.1016/0003-2697(79)90738-3

Ordy JM, Wengenack TM, Bialobok P, Coleman PD, Rodier P, Baggs RB, Dunlap WP, Kates B (1993) Selective vulnerability and early progression of hippocampal CA1 pyramidal cell degeneration and GFAP-positive astrocyte reactivity in the rat four-vessel occlusion model of transient global ischemia. Exp Neurol 119:128–139. https://doi.org/10.1006/exnr.1993.1014

Petschner P, Gonda X, Baksa D, Eszlari N, Trivaks M, Juhasz G, Bagdy G (2018) Genes linking mitochondrial function, cognitive impairment and depression are associated with endophenotypes serving precision medicine. Neuroscience 370:207–217. https://doi.org/10.1016/j.neuroscience.2017.09.049

Piantadosi CA, Zhang J (1996) Mitochondrial generation of reactive oxygen species after brain ischemia in the rat. Stroke 27:327–331 discussion 332

Picard M, McEwen BS (2014) Mitochondria impact brain function and cognition. Proc Natl Acad Sci 111:7–8. https://doi.org/10.1073/pnas.1321881111

Pulli B, Ali M, Forghani R, Schob S, Hsieh KLC, Wojtkiewicz G, Linnoila JJ, Chen JW, Johnson R (2013) Measuring Myeloperoxidase Activity in Biological Samples. PLoS ONE 8:e67976. https://doi.org/10.1371/journal.pone.0067976

Raval AP, Liu C, Hu BR (2009) Rat model of global cerebral ischemia: the two-vessel occlusion (2VO) model of forebrain ischemia. In: Chen J, Xu ZC, Xu X-M, Zhang JH (eds) Animal models of acute neurological injuries. Humana Press, Totowa, NJ, pp 77–86

Sancheti JS, Shaikh MF, Khatwani PF, Kulkarni SR, Sathaye S (2013) Development and validation of a HPTLC method for simultaneous estimation of L-glutamic acid and γ-aminobutyric acid in mice brain. Indian J Pharm Sci 75:716–721

Sanderson TH, Reynolds CA, Kumar R, Przyklenk K, Hüttemann M (2012) Molecular mechanisms of ischemia-reperfusion injury in brain: pivotal role of the mitochondrial membrane potential in reactive oxygen species generation. Mol Neurobiol 47:9–23. https://doi.org/10.1007/s12035-012-8344-z

Scaduto RC, Grotyohann LW (1999) Measurement of mitochondrial membrane potential using fluorescent rhodamine derivatives. Biophys J 76:469–477

Scarpulla RC (2011) Metabolic control of mitochondrial biogenesis through the PGC-1 family regulatory network. Biochim Biophys

Acta 1813:1269–1278. https://doi.org/10.1016/j.bbamcr.2010.09.019

Schaar KL, Brenneman MM, Savitz SI (2010) Functional assessments in the rodent stroke model. Exp Transl Stroke Med 2:13. https://doi.org/10.1186/2040-7378-2-13

Schimidt HL, Vieira A, Altermann C, Martins A, Sosa P, Santos FW, Mello-Carpes PB, Izquierdo I, Carpes FP (2014) Memory deficits and oxidative stress in cerebral ischemia–reperfusion: neuroprotective role of physical exercise and green tea supplementation. Neurobiol Learn Mem 114:242–250. https://doi.org/10.1016/j.nlm.2014.07.005

Sedlak J, Lindsay RH (1968) Estimation of total, protein-bound, and nonprotein sulfhydryl groups in tissue with Ellman's reagent. Anal Biochem 25:192–205. https://doi.org/10.1016/0003-2697(68)90092-4

Selakovic V, Korenic A, Radenovic L (2011) Spatial and temporal patterns of oxidative stress in the brain of gerbils submitted to different duration of global cerebral ischemia. Int J Dev Neurosci 29:645–654. https://doi.org/10.1016/j.ijdevneu.2011.02.009

Shaik IH, Mehvar R (2006) Rapid determination of reduced and oxidized glutathione levels using a new thiol-masking reagent and the enzymatic recycling method: application to the rat liver and bile samples. Anal Bioanal Chem 385:105–113. https://doi.org/10.1007/s00216-006-0375-8

Sims NR (1992) Energy metabolism and selective neuronal vulnerability following global cerebral ischemia. Neurochem Res 17:923–931

Tachibana M, Ago T, Wakisaka Y, Kuroda J, Shijo M, Yoshikawa Y, Komori M, Nishimura A, Makihara N, Nakamura K, Kitazono T (2017) Early Reperfusion After Brain Ischemia Has Beneficial Effects Beyond Rescuing Neurons. Stroke 48:2222–2230. https://doi.org/10.1161/STROKEAHA.117.016689

Wang X, Michaelis EK (2010) Selective neuronal vulnerability to oxidative stress in the brain. Front Aging Neurosci 2:12. https://doi.org/10.3389/fnagi.2010.00012

Yen LF, Wei VC, Kuo EY, Lai TW (2013) Distinct Patterns of Cerebral Extravasation by Evans Blue and Sodium Fluorescein in Rats. PLoS ONE 8:e68595. https://doi.org/10.1371/journal.pone.0068595

Zhou Y, Lian S, Zhang J, Lin D, Huang C, Liu L, Chen Z (2018) Mitochondrial perturbation contributing to cognitive decline in streptozotocin-induced type 1 diabetic rats. Cell Physiol Biochem 46:1668–1682. https://doi.org/10.1159/000489243

Publisher's note   Springer Nature remains neutral with regard to jurisdictional claims in published maps and institutional affiliations.